bladeRAD: Development of an Active and Passive, Multistatic Enabled, Radar System

Piers J. Beasley[1], Matthew A. Ritchie[2]
Department of Electronic and Electrical Engineering, University College London, UK
{[1]piers.beasley.19, [2]m.ritchie}@ucl.ac.uk

***Abstract*— In this paper the development of a hybrid active and passive experimental radar system utilising a low-cost Software Defined Radio is explored. The potential future evolution from monostatic to multistatic sensing is described and the synchronisation performance limitations of the system are summarised through a number of preliminary laboratory experiments. In addition, the first of a series of practical radar experiments are presented in order to verify the systems active and passive sensing modes.**

***Keywords*— Multistatic Radar, Software Defined Radio, FMCW Radar, Software Defined Radar, Passive Radar.**

I. Introduction

The topic of hybrid active passive radar is gaining more attention with a number of papers starting to surface on the expected benefits from the hybrid architecture [1], [2], [3]. A hybrid system can capitalise on the strengths of passive radar (PR) (e.g. zero transmitter cost, covert operation), as well as the strengths of active radar (e.g. optimised waveform, transmit beam-steering). However, little is published on the design of such a system, and therefore few empirical results have been reported to concretely support the claimed performance enhancements. Until now, the complexity and cost of implementing a hybrid system will likely have been a limiting factor. With the recent advancements of Software Defined Radio (SDR) technology, SDRs now provide low-cost highly flexible platforms that can be used to perform the multiple functions at multiple frequency bands required of a hybrid radar system.

As the capability and accessibility of SDRs has increased, research into the exploitation of SDRs in radar applications has become more prevalent. One particular SDR, the Universal Software Radio Peripheral (USRP), is used in a large quantity of the published work on SDR radar. A good example of the use of the USRP in a PR system can be found in [4], [5], where researchers from the University of Cape Town develop an FM PR system to successfully detect aircraft flying into Capetown International Airport. Additionally, an example of an active system, developed around a USRP NI2920, can be found in [6], where an Frequency Modulated Continuous Wave (FMCW) system was verified for a limited set of short range experiments detecting static targets at ranges up to 12m. As the technology continues to mature, more SDRs of comparable performance to the USRP are becoming available, but for a fraction of the cost e.g. bladeRF xA4, LimeSDR and RTL-SDR.

This paper presents the development of an experimental hybrid active passive radar system utilising one of these low-cost high-performance SDRs. The architecture of the hybrid system is introduced before, presenting empirical results for transmitter (TX) to receiver (RX) synchronisation. In section III the future evolution from the monostatic system, described section II, to a multistatic system is briefly explained. Section IV reviews some preliminary active and passive results. In the final section, a conclusion of the work is presented along with a plan for future work.

II. SDR Based Active Passive Radar System

The Nuand bladeRF micro 2.0 xA4 is a low-cost highly versatile SDR available to purchase for approximately 480 USD. A cross comparison between with a selection of comparably priced SDRs found the bladeRF xA4 to be most suitable for the purpose of multi-functional multi-frequency radar applications. Of co rable interest, is the bladeRF's high central RF limit c Hz, surpassing the LimeSDR, XTRX CS, bladeRF x40 and KerberosSDR. The bladeRF xA4 hosts the AD9361 transceiver RFIC, capable of 2 X 2 MIMO operation with channel bandwidths dynamically selective between 0.2MHz to 56 MHz, making the SDR particularly suitable for hybrid radar applications. An evaluation of the bladeRF xA4's predecessor, the bladeRF x40, for use in Stepped Frequency Continuous Wave (SFCW) Radar can be found in [7], [8]. Though the x40 uses a different LMS6002D RFIC. A more recent publication [9], assesses the use of an xA4 SDR as an SFCW radar for breast screening exams, where a detailed evaluation of the xA4's TX and RX performance over its entire RF range can be found. The focus of this paper is to evaluate the architecture of a hybrid radar system, and present some initial experimental results using the developed solution.

1) bladeRF CLI

In this work, the vendor supplied bladeRF Command Line Interface (CLI) running on a host PC was used to administer control to the SDR through the USB 3.0 interface. The CLI allows access to the majority of the SDR's functionality including, importantly, the ability to synchronously stream TX and RX channels between the SDR and PC. This is fundamental for radar signal processing. When using the bladeRF CLI to simultaneously stream TX and RX channels, the bandwidth of the USB 3.0 interface was found

to considerably limit the maximum cumulative bandwidths achievable with the four SDR channels (there is a widely understood full-duplex bandwidth limit of 40 MSPS between SDR and PC [9]).

A. Monostatic Radar Transceiver

When developing an active radar transceiver using the bladeRF, considerable buffering issues resulting from bandwidth constraints of the USB 3.0 interface were avoided by splitting the TX and RX streams across two separate SDRs. In this configuration a 40MHz transceiver bandwidth was verified, by connecting both the TX SDR and RX SDRs to the same Dell XPS laptop running Ubuntu. Given this bandwidth, B, the attainable transceiver range resolution, ΔR, can be calculated to be 3.75m, using equation (1). Where v is the speed of light in Earth's atmosphere.

$$\Delta R = \frac{v}{2B} \tag{1}$$

1) Signal Processing

Due to the waveform versatility of the SDR, the transceiver is capable of both FMCW and Pulse-Doppler radar sensing. In both radar modes all radar signal processing is done post capture in MATLAB®. When using the radar in FMCW mode, unlike conventional hardware defined FMCW radars, deramping of the receive channel is done post capture in DSP using a prerecorded FMCW chirp, see Fig.1.

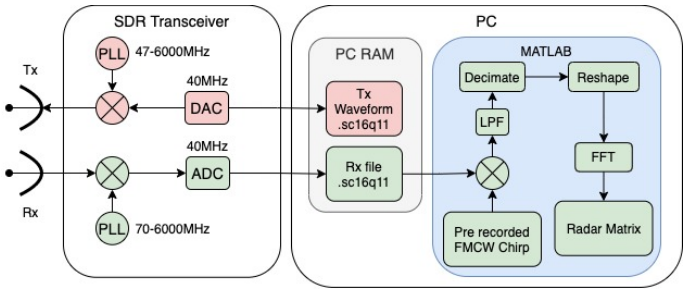

Fig. 1. Simplified signal processing flow of bladeRF based monostatic FMCW radar transceiver.

2) Transmitter and Receiver SDR Synchronisation

The bladeRF xA4 has the external control inputs and internal circuitry required to synchronise TX and RX events across multiple bladeRF SDRs. The start of acquisitions can be synchronously triggered by sharing a trigger signal from the TX SDR to RX SDR, see Fig. 2. Additionally, the TX SDR can also share its 38.4MHz Voltage Controlled Temperature Compensated Crystal Oscillator (VCTCXO) with the RX SDR in order to synchronise the DACs, ADCs and data clocks across the two boards. In this configuration the RX SDR uses the TX SDR's VCTCXO signal in the place of its own, see Fig.2. This functionality, allows multiple SDRs to be used in parallel with the equivalent baseband performance to a single device.

3) Radar Trigger Accuracy

Trigger error will only impact the start of the TX/RX acquisition, though will result in a constant target range estimation error for the continuation of the capture. An experiment was conducted to test the trigger accuracy of the transceiver. This was done by transmitting a single pulse from the TX port to the RX port via a 40m RF cable. The 40m RF cable was used in order to delay the pulse, simulating a stationary target at a know fixed range. The results from 200 trigger experiments are presented in Fig. 3. It was found that the trigger performance resulted in zero range error for 62% of triggers, and a ±1 range bin error for 37.5% of triggers. This error results from the method in which the triggers are setup on the FPGA using the bladeRF CLI.

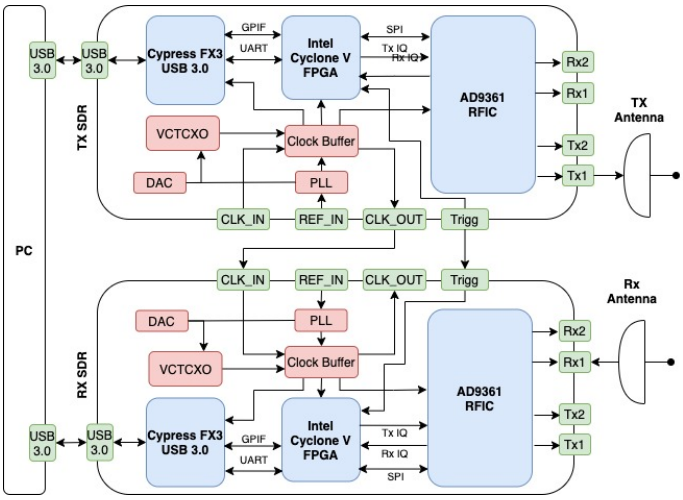

Fig. 2. bladeRF based monostatic FMCW radar transceiver. Comprising of two bladerRF xA4 SDRs, one acting as TX and the other RX. Acquisition synchronisation achieved through sharing of a trigger signal from TX SDR's FPGA to RX SDR's FPGA. Baseband sampling synchronisation achieved through sharing of 38.4MHz VCTCXO from TX SDR to RX SDR.

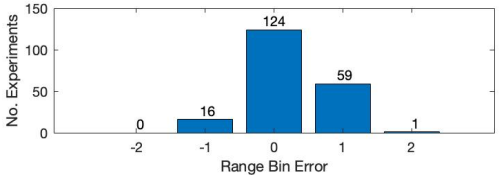

Fig. 3. Stationary target range bin errors resulting from radar trigger inaccuracy between TX and RX streams. Results gathered for 200 trigger events in FMCW mode.

4) Monostatic Radar Phase Measurement

Self-loop tests using a 40m section of RF cable were performed to verify the transceivers phase stability in the Doppler domain through long recordings. Though baseband operations are synchronised across multiple SDRs, the bladeRF does not contain the internal circuitry required for phase coherent RF operations. That said, both TX and RX RF PLLs, used for pass-band mixers, are derived from a common VCTCXO. Therefore, we should expect the RFs to be coherent, yet exhibit a random constant relative phase offset. The phase

stability of a 2.4GHz central frequency was evaluated over a 120s period by connecting TX and RX port via a 40m RF cable in order to simulate a stationary target at a known fixed range. After identifying the range bin containing the pseudo target, the phase series was attained by taking the argument of the complex samples down the slow-time dimension of the radar matrix. The phase series was then unwrapped to remove 2π discontinuities. Fig.4 illustrates the phase series for two identical 120s experiments. The results from both experiments were first normalised to zero, before the second experiments phase series was then offset by 0.1 radians. In the first 15s of both captures an initial phase excursion, of in the most extreme case 0.12 radians, can be observed. The cause of this excursion is not yet fully understood. However, for the continuation of the capture a net phase drift of < 0.05 radians (2.87 Hz) is observed in both results. Indicating an RF synchronisation error of $< 79.6 \times 10^{-6}$Hz, resulting in a negligible target Doppler velocity error. The coherent integration loss resulting from the phase noise can be calculated from the phase series variance using Richards' analytic expression [10]. The worst case variance was found to be 4.30×10^{-4} radians, resulting in an inconsequential coherent integration loss of 8.04×10^{-7}dB.

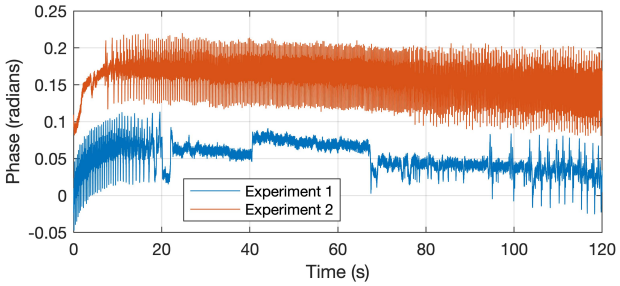

Fig. 4. 2 Minute 5kHz PRF monostatic radar phase series of pseudo stationary target for two identical 2.4GHz experiments. TX and RX channels connected via 40m RF cable.

B. Passive Radar Receiver

The bladeRF's two receive channels make it suitable for use as a PR receiver: one for sampling the direct path from a IO, and the other for sampling IO reflections from targets. In addition, the frequency agility of the receive channels also make it suitable for use with a variety of Illuminators of Opportunity (IO). Though, the results presented in this paper are limited to using a 2.4GHz Wi-Fi IO. The active transceiver in section II-A can be developed into a hybrid system through the simple addition of a third SDR for purely passive sensing. In this work, the reference and surveillance channels are processed in MATLAB® using a batched PR processing algorithm as described by Bo Tan et al in [11].

III. Multistatic Radar System

The hybrid radar system evaluated in the previous section can be further developed into a multistatic system through disciplining multiple radar nodes to a common external trigger and frequency reference. The bladeRF SDR features a secondary method for clock synchronisation of multiple boards, by utilising the on-board ADF4002 PLL to discipline its VCTCXO to an external frequency reference. This feature allows common frequency reference sources such as GPSDOs to be used to synchronise spatially separated SDRs. A GPSDO radar synchronisation system has been developed in parallel with the work described in this paper. The purpose of this system is to provide synchronous trigger and frequency references to spatially separated radar nodes, removing the requirement for physical synchronisation cables. The final paper submission will include: further details on the method for time and frequency distribution; bladeRAD's multistatic performance limitations.

IV. Active Passive Radar Experiments

In this section, a series of active and PR results are presented from experiments using the multi-functional radar system introduced in Section II. The experiments were conducted in a small laboratory environment, illustrated in Fig.5, using either a human or micro-drone as a radar target.

For the active experiments the system was setup in FMCW mode with a central frequency of 2.45GHz using the monostatic transceiver configuration detailed in II-A. Though the bladeRF is capable of a 8dBm CW ouput power at 1GHz, the max output power at 2.45GHz is 0dBm. A saw-tooth waveform with a bandwidth of 40MHz and PRF of 5kHz was selected. Both TX and RX channels were connected to 18dBi parabolic dish antennas via 2.4GHz ISM pass-band filters. For PR experiments, an Archer C9 Wi-Fi Access Point (AP) was used as an IO. A 20MHz 802.11n Wi-Fi channel, centred on on a 2.437GHz, with a power of 20dBm was configured. The Wi-Fi channel was stimulated using the MGEN network traffic generator tool [12]. 18dBi parabolic dish antennas were again used for both reference and surveillance channels.

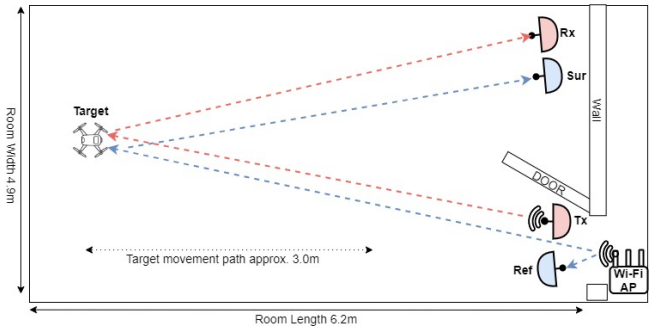

Fig. 5. Experimental setup for active and passive laboratory experiments. Antenna locations and orientations for active FMCW radar experiments and Wi-Fi based PR experiments are indicated by red filled antennas and blue filled antennas respectively.

1) Human Target

The first results presented are of a human walking directly back and forth from the radar. Vertical antenna polarisation were selected for both radar modes. Following the necessary radar signal processing, a single delay line Moving Target Indicator (MTI) was implemented in the active radar data to discriminate the moving target from the considerable stationary

clutter. Fig. 6. details the spectrogram results for the active and passive radar captures. The Doppler shift contribution from the radial movement of the human's torso can be observed at ±20 Hz in both FMCW and PR results. In the active result, the periodic streaks of Doppler centered around the bulk Doppler are associated to the free swinging movements of the human's limbs. These periodic streaks represent the characteristic micro-Doppler signature of a human's gait [13].

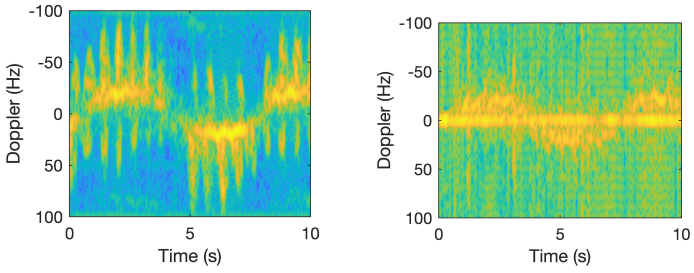

Fig. 6. Spectrogram results for human target walking back and forth from active and passive radar. Spectrogram window duration of 0.2s, with 90% overlap and zero padding factor of 4. (a) result for S-Band FMCW Radar; (b) result for Wi-Fi PR capture

2) *Micro-Drone Target*

The next result presented is for a DJI Spark micro-drone flying slowly back and forth from the radar. In this experiment horizontal polarisation of antennas was selected. Additionally, in order to overcome the considerable interference introduced by the micro-drones 2.4GHz radio control system, a power amplifier was introduced in to the FMCW radars TX chain, increasing the TX power to 19dBm. The Spectrogram result for the active experiment is detailed in Fig. 7. Helicopter Rotor Modulation (HERM) lines can be observed with a spacing of ±400Hz around the micro-drone's bulk Doppler. HERM lines result from the micro-motion of the micro-drone's propellers and exhibit a frequency spacing equal to the number of blades per propeller, multiplied by the propeller rotational rate [14]. In the final paper submission, direct signal interference cancellation will be operated on the passive radar results to better expose both targets' micro-Doppler signatures; a passive result will then also be included for the micro-drone.

V. Conclusion

In this paper, the 'bladeRAD' hybrid radar system developed with a combination of synchronised low-cost bladeRF xA4 SDRs is presented. In section II the TX to RX SDR synchronisation is evaluated, and the RF phase error is found to result in negligible Doppler offsets at a 2.4GHz RF. The impact of triggering errors between SDRs is also presented, where the error is limited to ±1 range bin for 99.5% of acquisitions. However, it is thought this error could be rectified in post processing using the back-scatter from a stationery clutter reference at a known fixed range. Section IV reports some preliminary results for active and passive sensing of both a human and micro-drone, though the results are limited to frequency domain analysis, due to the limited radial motion of the target in relation to the radar's range resolution. Future work will focus on the development of bladeRAD into a multistatic system, at which point further experiments will be conducted for larger target ranges and a variety of multistatic scenarios.

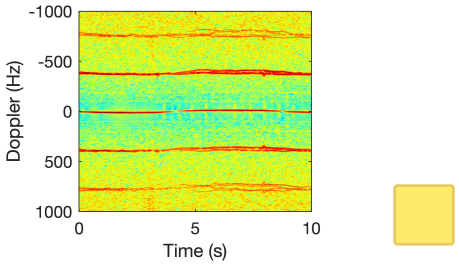

Fig. 7. Spectrogram result for micro-drone target flying back and forth from S-Band FMCW Radar. Spectrogram window duration of 0.2s, with 90% overlap and no zero padding.

References

[1] F. Wang and H. Li, "Joint waveform and receiver design for co-channel hybrid active-passive sensing with timing uncertainty," *IEEE Transactions on Signal Processing*, vol. 68, pp. 466–477, 2020.

[2] H. Kuschel, J. Heckenbach, and J. Schell, "Deployable multiband passive/active radar for air defense (dmpar)," *IEEE Aerospace and Electronic Systems Magazine*, vol. 28, no. 9, pp. 37–45, 2013.

[3] Y. Gao, H. Li, and B. Himed, "Joint transmit and receive beamforming for hybrid active-passive radar," *IEEE Signal Processing Letters*, vol. 24, no. 6, pp. 779–783, 2017.

[4] S. Heunis, Y. Paichard, and M. Inggs, "Passive radar using a software-defined radio platform and opensource software tools," in *2011 IEEE RadarCon (RADAR)*, May 2011, pp. 879–884.

[5] C. Tong, M. Inggs, and G. Lange, "Processing design of a networked passive coherent location system." IEEE, 2011, pp. 692–697.

[6] S. Costanzo, F. Spadafora, A. Borgia, H. O. Moreno, A. Costanzo, and G. Di Massa, "High resolution software defined radar system for target detection," *Journal of electrical and computer engineering*, vol. 2013, pp. 1–7, 2013.

[7] J. Marimuthu, K. S. Bialkowski, and A. M. Abbosh, "Stepped frequency continuous wave software defined radar for medical imaging," in *2014 IEEE Antennas and Propagation Society International Symposium (APSURSI)*, July 2014, pp. 1909–1910.

[8] K. Takahashi and T. Miwa, "Near-range sfcw uwb radar based on low-cost software defined radio," in *2019 IEEE Radar Conference (RadarConf)*, April 2019, pp. 1–6.

[9] D. Carvalho, A. J. Aragão, A. Ferrari, B. Sanches, and W. Noije, "Software-defined radio assessment for microwave imaging breast cancer detection," in *2020 IEEE Nordic Circuits and Systems Conference (NorCAS)*, Oct 2020, pp. 1–6.

[10] M. Richards, "Coherent integration loss due to white gaussian phase noise," *IEEE signal processing letters*, vol. 10, no. 7, pp. 208–210, 2003.

[11] B. Tan, K. Woodbridge, and K. Chetty, "A real-time high resolution passive wifi doppler-radar and its applications," 2014.

[12] R. B. Adamson, *MGEN-3.0 User's Guide*, U.S. Naval Research Laboratory, 2021. [Online]. Available: http://www-hera-b.desy.de/subgroup/network/mgen/UserGuide.html

[13] F. Fioranelli, M. Ritchie, and H. Griffiths, "Analysis of polarimetric multistatic human micro-doppler classification of armed/unarmed personnel," 2015.

[14] P. Beasley, M. Ritchie, H. Griffiths, W. Miceli, M. Inggs, S. Lewis, and B. Kahn, "Multistatic radar measurements of uavs at x-band and l-band," in *2020 IEEE Radar Conference (RadarConf20)*, Sep. 2020, pp. 1–6.